



Insights into the spatial distribution of global, national, and subnational greenhouse gas emissions in the Emissions Database for Global Atmospheric Research (EDGAR v8.0)

Monica Crippa², Diego Guizzardi¹, Federico Pagani², Marcello Schiavina⁶, Michele Melchiorri¹, Enrico Pisoni¹, Francesco Graziosi¹, Marilena Muntean¹, Joachim Maes⁵, Lewis Dijkstra^{1,5}, Martin Van Damme^{3,4}, Lieven Clarisse³, and Pierre Coheur³

¹European Commission, Joint Research Centre (JRC), Ispra, Italy

²Unisystems S.A., Milan, Italy

³Université libre de Bruxelles (ULB), Spectroscopy, Quantum Chemistry and Atmospheric Remote Sensing (SQUARES), Brussels, Belgium

⁴Royal Belgian Institute for Space Aeronomy (BIRA-IASB), Brussels, Belgium

⁵European Commission, Directorate-General for Regional and Urban Policy, Brussels, Belgium

⁶NTT DATA, Rue de Spa 8, 1000 Brussels, Belgium

Correspondence: Enrico Pisoni (enrico.pisoni@ec.europa.eu)

Received: 11 December 2023 – Discussion started: 14 December 2023

Revised: 12 April 2024 – Accepted: 15 April 2024 – Published: 14 June 2024

Abstract. To mitigate the impact of greenhouse gas (GHG) and air pollutant emissions, it is of utmost importance to understand where emissions occur. In the real world, atmospheric pollutants are produced by various human activities from point sources (e.g. power plants and industrial facilities) but also from diffuse sources (e.g. residential activities and agriculture). However, as tracking all these single sources of emissions is practically impossible, emission inventories are typically compiled using national-level statistics by sector, which are then downscaled at the grid-cell level using spatial information. In this work, we develop high-spatial-resolution proxies for use in downscaling the national emission totals for all world countries provided by the Emissions Database for Global Atmospheric Research (EDGAR).

In particular, in this paper, we present the latest EDGAR v8.0 GHG, which provides readily available emission data at different levels of spatial granularity, obtained from a consistently developed GHG emission database. This has been achieved through the improvement and development of high-resolution spatial proxies that allow for a more precise allocation of emissions over the globe.

A key novelty of this work is the potential to analyse subnational GHG emissions over the European territory and also over the United States, China, India, and other high-emitting countries. These data not only meet the needs of atmospheric modellers but can also inform policymakers working in the field of climate change mitigation. For example, the EDGAR GHG emissions at the NUTS 2 level (Nomenclature of Territorial Units for Statistics level 2) over Europe contribute to the development of EU cohesion policies, identifying the progress of each region towards achieving the carbon neutrality target and providing insights into the highest-emitting sectors. The data can be accessed at <https://doi.org/10.2905/b54d8149-2864-4fb9-96b9-5fd3a020c224> specifically for EDGAR v8.0 (Crippa et al., 2023a) and <https://doi.org/10.2905/D67EEDA8-C03E-4421-95D0-0ADC460B9658> for the subnational dataset (Crippa et al., 2023b).

1 Introduction

Knowing where emissions are released is essential to supporting the design of effective mitigation actions and for atmospheric modelling purposes. Emission inventories are typically developed at the national level and provide sector-specific emission estimates. In order to disaggregate national emissions over high-resolution grids, information on the location of the different emission sources (e.g. point, linear, and area sources) must be collected, and “spatial proxies” should be developed and applied to national sector-specific emission totals to downscale them over grid maps. The correct allocation of point source emissions is essential to avoid misplacing high emission levels. However, gathering information on point sources covering the entire globe and a wide temporal domain (1970 to present) is challenging because of limitations in data availability, in the accuracy of the reporting (real location vs. legal address, etc.), and in the completeness of data.

The Emissions Database for Global Atmospheric Research (EDGAR) provides global greenhouse gas (GHG) and air pollutant emissions over the global grid map at a $0.1^\circ \times 0.1^\circ$ resolution, obtained through a downscaling process of national emissions using high-resolution spatial data. The development and maintenance of the EDGAR grid maps is essential since several regional and global databases rely on the EDGAR emission grid maps to disaggregate national emissions to the grid. This is the case for the Community emissions data system (Feng et al., 2020; Hoesly et al., 2018) or the European Monitoring and Evaluation Programme (EMEP) Centre on Emission Inventories and Projections (CEIP), which supports Parties to the Convention on Long-range Transboundary Air Pollution in meeting their official gridded emission reporting obligations (CEIP, 2021).

This work is an update of previous EDGAR publications dealing with spatial data (Janssens-Maenhout et al., 2019; Crippa et al., 2021) and describes all the new developments in the spatialisation of the emissions from EDGAR v8.0 onwards, focusing on not only high-emitting sectoral point sources, such as power plants and industrial activities, but also more diffuse sources, such as residential activities. High-resolution spatial information has been gathered at the global level by combining data from the Global Energy Monitor, official registries, and satellite retrievals. The relevance of using updated spatial information is also assessed through regional case studies.

The purpose of this publication is to describe the EDGAR v8.0 GHG gridded emission datasets, focusing on the updates to the spatial proxies included in this data release. The analysis of EDGAR v8.0 emission time series (European Union, 2023; IEA-EDGAR CO₂, 2023) and the methodology behind emission calculations are available in Crippa et al. (2023c).

The main novelties of this work are (i) an update on emission point sources using global datasets (e.g. Global Energy Monitor), (ii) the development of a gap-filling method

for non-population-based sources using built-up surface information for non-residential areas¹ from the Global Human Settlement Layer (GHSL), (iii) an update of population-based proxies using the latest GHSL data, including a weighting for the temperature-dependent need for heating, and (iv) an update on international ship tracks and weights by vessel type. In addition, information at the subnational level (e.g. for Europe at the Nomenclature of Territorial Units for Statistics level 2, NUTS 2 level) is included when developing the new spatial proxies for EDGAR, thus allowing for a more accurate allocation and analysis of subnational emissions. The EDGAR v8.0 GHG global emission maps can be accessed at <https://doi.org/10.2905/D67EEDA8-C03E-4421-95D0-0ADC460B9658> (Crippa et al., 2023b) for the subnational emissions and at <https://doi.org/10.2905/b54d8149-2864-4fb9-96b9-5fd3a020c224> (Crippa et al., 2023a) for v8.0 and the emission grid maps at a $0.1 \times 0.1^\circ$ resolution.

2 Overview of the methodology and data sources used for updating spatial information in EDGAR

Bottom-up global inventories (such as EDGAR) compute emissions for each sector, pollutant, and year at the national level, making use of international statistics and official guidelines for emission computation (Janssens-Maenhout et al., 2019; Crippa et al., 2018). However, atmospheric modellers, policymakers, local authorities, and scientists may need to analyse spatially distributed emissions at a higher resolution than country-level data. Therefore, annual country-specific emissions are distributed over the globe, making use of spatial information and representing the exact location of point sources (e.g. power plants and industrial facilities), linear tracks (e.g. road network, ship, and aeroplane tracks), or area sources (e.g. populated areas and industrial areas). Within the EDGAR database, over 130 proxy datasets (f) varying over time have been developed to distribute the contribution of sector-specific emissions ($EM_{i,j,k}$) of each country (C) and pollutant (x) over time (t) to each grid cell ($em_{i,j,k}$) at a $0.1^\circ \times 0.1^\circ$ resolution (about 10 km spatial resolution at the Equator, considering the World Geodetic System 1984, WGS84, EPSG:4326). The Heaviside function (i.e. unit step function whose value is 0 for negative arguments and 1 for positive arguments) is also used, equalling 1 when the grid cell belongs to the country area, accordingly with the following formula:

¹This information is compliant with the definition of “building” as per the Infrastructure for Spatial Information in Europe (INSPIRE) directive (<https://inspire.ec.europa.eu/id/document/tg/bu>, last access: June 2024) for non-residential areas (e.g. industrial or commercial facilities and warehouses) from the Global Human Settlement Layer.

$$em_{i,j,k}(\text{lon}, \text{lat}, t, x) = EM_{i,j,k}(C, t, x) \cdot \frac{f_{i,j,k}(\text{lon}, \text{lat}, t)}{\sum_{\text{lon}, \text{lat}} (f_{i,j,k}(\text{lon}, \text{lat}, t) \cdot H_{i,j}(C, \text{lon}, \text{lat}))}, \quad (1)$$

where $H_{i,j}(C, \text{lon}, \text{lat})$ is the fraction and/or weight of grid cell within C , i the sector, j the fuel, and k the technology.

Table 1 summarises the data sources and the methodology used to update spatial information for each emitting sector in the EDGAR database, highlighting the most relevant and latest updates compared with previous EDGAR data releases. These updates apply from EDGAR v8.0 onwards. Being a global database of emissions, the spatial data sources are typically developed at the global level (e.g. satellite-based retrievals) but often rely on national data collection (e.g. national point source information reported to fulfil legal requirements). Therefore, the same data sources may be used by other inventory developers to update their spatial disaggregation of the emission data. In the following sections, a detailed description of the data sources and the approach used for updating each emission sector is provided, distinguishing between point sources, area sources, and linear sources. For all sectors not subject to a recent revision in the EDGAR database, we refer the reader to the overview in Table S1 in the Supplement and the references therein.

A key methodological advance in the EDGAR gridding system is the inclusion of subnational attributes for each spatial proxy and, in particular, for each point source. This implies attaching to each point not only its exact location, expressed in longitude and latitude, but also the related NUTS 2 code (EUROSTAT, 2021) for Europe or the Global Administrative layer at level 1 (GADM version 4.1). The decision to include NUTS 2 rather than NUTS 3 information aims to enhance the capability of a global database such as EDGAR to represent subnational regional emissions in support of the development of regional policies (e.g. EU cohesion reports; European Union, 2022, 2024) or the 2040 climate impact assessment. The attribution of subnational details is developed not only with an EU-oriented focus, but also for other countries such as China, India, and the United States by providing emissions at the state or province level.

The purpose of our work is to provide readily available emission data at the subnational level estimated in a consistent way for all countries. The EDGAR data may represent an approximation for those countries with a developed statistical infrastructure (e.g. those including subnational statistics and very precise spatial proxies); however, they provide a default if such data are not available, as is the case for many countries in the world. In the results section, case studies on subnational emissions are presented for the EU, China, India, and the United States.

3 Point sources of emissions

Gathering information on point sources covering the globe and spanning a wide temporal domain (1970 to present) is challenging because of the limited data available and their accuracy and completeness in the reporting (real plant location vs. legal address, etc.). Establishing the correct location of point sources is essential since they are often super-emitters (e.g. power plants for CO₂ emissions). In EDGAR v8.0, the locations of the main industrial point sources (e.g. power plants, iron and steel industries, coal mines, and venting and flaring activities), which contribute around half of global CO₂ emissions, have been updated using state-of-the-art information from global databases, such as the Global Oil and Gas Plant Tracker and Global Coal Plant Tracker of the Global Energy Monitor. A complete overview of the data sources and updates included in EDGAR v8.0 is provided in Table 1.

However, point source databases are characterised by some limitations, such as the completeness of information on the point sources, the availability of time series for information, and the misplacement of data points compared with their actual country location. In EDGAR v8.0, quality control procedures are applied to validate the correct location of each point source to the corresponding country or subnational attribute. Moreover, missing information is provided using assumptions on the lifetime of power plants (i.e. 40 years) to indicatively attribute the opening or closing years for each plant.

No consistency checks between CO₂ emissions estimated using independent methods have been performed here. However, Guevara et al. (2024) have proven that there is good agreement between national CO₂ emissions from power plants reported by EDGAR (which are based on international statistics) and plant-level inventories.

Atmospheric modellers require information on not only the spatial patterns of the emissions but also their temporal and vertical distribution, as described in Ahsan et al. (2023), Bieser et al. (2011), and de Meij et al. (2006). For example, de Meij et al. (2006) found that the vertical distribution of emissions of SO₂ and nitrogen oxides (NO_x) plays an important role in understanding the differences between emission inventories in calculated gas and aerosol concentrations. Accordingly, in the EMEP model, industrial point source and power plant emissions occur up to the third level (up to 184 m), while shipping emissions happen in the first level (up to 20 m). However, addressing the vertical distribution of the emissions is beyond the scope of this work. In the following sections, we will describe, sector by sector, how the most up-to-date spatial data on point sources have been collected and implemented in the EDGAR database to down-scale national emissions over the global grid map.

Table 1. Overview of updated spatial proxies in EDGAR v8.0, including data sources and methods.

| Sector and spatial coverage | Old EDGAR proxies | New EDGAR proxies | Details of new EDGAR proxies | Period covered | Data access (last access: June 2024) |
|--|---|--|---|---|---|
| Power plants (global) | CARMA v3.0 (no longer available; for 2004, 2009, 2014), fuel type derived from plant capacity (assumption) | Global Coal, Gas and Oil Plant Tracker (Global Energy Monitor) | Coal, gas | 1970–2050 | https://globalenergymonitor.org/projects/global-coal-plant-tracker/ and https://globalenergymonitor.org/projects/global-gas-plant-tracker/ (2022) |
| | | Global Power Plant Database v1.3.0 | Biomass, other, oil | | https://datasets.wri.org/dataset/globalpowerplantdatabase |
| | | US EIA | USA power plants, all fuels | 1970–2021 | https://atlas.eia.gov/datasets/eia::power-plants/explore?location=41.629235%2C-118.496000%2C3.79 |
| | | CARMA v3.0 | Autoproducers, missing countries | 2004, 2009, 2014 | Ummel (2012) |
| All other industries (Europe) | E-PRTR v4.2 | E-PRTR v18 | All industries and waste plants (with the exception of power plants, iron and steel plants, and coal mines) | 2007–2017 | https://www.eea.europa.eu/data-and-maps/data/member-states-reporting-art-7-under-the-european-pollutant-release-and-transfer-register-e-prtr-regulation-23/european-pollutant-release-and-transfer-register-e-prtr-database/eprtr_v9_csv.zip |
| Iron and steel (global) | In-house EDGAR | Global steel plant tracker (Global Energy Monitor) | | 1970–2050 | https://globalenergymonitor.org/projects/global-steel-plant-tracker/ |
| Coal mines (global) | USGS-derived proxies, Global Energy Observatory (China) | Global Coal Mine Tracker (Global Energy Monitor) | Brown and hard coal, surface and underground | 1970–2050 | https://globalenergymonitor.org/projects/global-coal-mine-tracker/ |
| | | Global Energy Monitor and EIA | United States, all fuels, more precise opening and closing years | 1970–2050 | https://atlas.eia.gov/datasets/eia::coal-mines-1/explore |
| | | EDGAR old proxy | For missing countries | Key years | |
| Flaring (global) | NOAA-NGDC (2017) VIIRS data (https://www.ngdc.noaa.gov/eog/viirs.html) | Global Gas Flaring Tracker Report (2023) | Used for both venting and flaring activities | 2012–2022 | https://www.worldbank.org/en/programs/gasflaringreduction/global-flaring-data |
| Small-scale combustion (global) | GHSL (for 1975, 1990, 2000, 2015) | GHSL Data Package 2023 and HDDs from ERA5 | For all fuels | Population every 5 years from 1975 to 2030, HDDs every year from 1970 to 2022 | https://ghsl.jrc.ec.europa.eu/ghs_pop2023.php and https://cds.climate.copernicus.eu/cdsapp#!/dataset/reanalysis-era5-single-levels?tab=form |
| Small-scale combustion in agriculture (global rural population) | GHSL (for 1975, 1990, 2000, 2015) | GHSL Data Package 2023, including GHSSMOD R2023A – GHS settlement layers and HDDs from ERA5 | For small-scale combustion in agriculture, which is mostly associated with rural areas | Rural population every 5 years from 1975 to 2030, HDDs every year from 1970 to 2022 | https://ghsl.jrc.ec.europa.eu/ghs_pop2023.php , https://ghsl.jrc.ec.europa.eu/ghs_smod2023.php , and https://cds.climate.copernicus.eu/cdsapp#!/dataset/reanalysis-era5-single-levels?tab=form) |
| Intensive livestock and fertiliser-manufacturing industries (global) | Livestock density maps | European Space Agency World Emission project and intensive livestock point sources were taken from E-PRTR v18 for Europe | For intensive livestock and fertiliser industry and gap filling with a livestock density map | 2008–2022 | https://www.world-emission.com/ |

Table 1. Continued.

| Sector and spatial coverage | Old EDGAR proxies | New EDGAR proxies | Details of new EDGAR proxies | Period covered | Data access (last access: June 2024) |
|---|--|--|--|---------------------------------|---|
| Gap filling of industrial activities (global) | Population-based | Built up for non-residential areas from GHSL Data Package 2023 | Used throughout when no information is available or for attributing a fraction of emissions that is not allocated to point sources | Every 5 years from 1975 to 2030 | https://ghsl.jrc.ec.europa.eu/ghs_buS2023.php |
| International shipping | In-house EDGAR proxy based on long-range identification and tracking and Wang et al. (2008) and Alessandrini et al. (2017) | STEAM | Based on CO ₂ emissions for multiple vessels and multiple years | 2000–2018 | Jalkanen et al. (2012), Johansson et al. (2017) |

3.1 Power plants

Power plants represent a major source of fossil-fuel-derived CO₂ and other GHG emissions globally, nowadays contributing around 38 % and 18 %, respectively, of the corresponding global totals (Crippa et al., 2023c). It is therefore of utmost importance to spatially allocate these emissions correctly at the global level and understand their trends over time in order to design and implement adequate emission mitigation measures.

In EDGAR v8.0, fuel-specific spatial proxies have been developed using data from the Global Coal Plant Tracker and Global Oil and Gas Plant Tracker of the Global Energy Monitor (for coal and gas) (Global Energy Monitor, 2022b, c), the Global Power Plant Database v1.3.0 (World Resources Institute, 2018; WRI, 2021) for oil and biofuels, and the Carbon Monitoring for Action database (CARMA v3.0) for autoproducers (i.e. plants and industries producing power for their own use). In addition, information on autoproducers and biofuel-fired power plants in Europe has been integrated using the European Pollutant Release and Transfer Register (E-PRTR v18) (European Union, 2022). For the US domain, the location of fossil-fuel-fired power plants is taken from the US Energy Information Administration (US EIA, 2022b) as it represents the most up-to-date source for the United States. The time frame covered by the new power plant spatial proxy datasets developed in EDGAR v8.0 is 1970–2022, which includes, for each plant, information on opening and closing years (including beyond 2022 for recently built power plants), capacity, and main fuel type. When only partial information is available for the years of operation, assumptions based on the typical lifetime of power plants (e.g. 40 years) are made. The capacity of each power plant is used to relatively weight the fuel-specific emissions from power plants within a country. An additional adjustment is performed for the US data to account for the different sulfur content in the fuel used in different US states based on EIA and Federal Energy Regulatory Commission utility surveys.

The Global Energy Monitor is chosen as the main data source for updating power plant proxies since it relies on data from public and private data sources (including the Global Energy Observatory, CARMA, Platts World Electric Power Plants database, national-level trackers developed by environmental organisations, and various company and government sources). It is validated with (i) government data on individual power plants, (ii) country energy and resource plans and government websites tracking coal plant permits and applications, (iii) reports by state-owned and private power companies, (iv) news and media reports, and (v) local non-governmental organisations tracking coal plants or permits. Local experts are also involved in the review of coal and gas plant data. Regular biannual updates of these databases also guarantee the possibility of including further updates in future EDGAR releases. As of January 2019, the Global Coal Plant Tracker included the exact locations of 95.3 % of operating units (6411 out of 6725). Independent use and validation of the Global Coal Plant Tracker and Global Oil and Gas Plant Tracker is also performed by Guevara et al. (2024). Figure S1 in the Supplement shows the comparison between the geographical coverage of EDGAR v8.0 and the previous EDGAR spatial data for power plants, while Fig. S2 provides a view of the global coverage of power plants in EDGAR v8.0 by fuel type.

Figure 1 shows the global coverage and intensity of CO₂ emissions from fossil-fuel-fired power plants from EDGAR v8.0 for the years 1970 and 2022. As a general trend, the number of power plants increased strongly from 1970 to 2022 (see also Fig. 2) due to global industrialisation over those 5 decades, although the number of power plants in 1970 is more uncertain than that for the present day.

The total number of power plants grew from around 8500 in 1970 to 13 000 in 2022, with the sharpest increases occurring in China (4.5 times more) and North America (2 times more). However, the intensity of the emissions has changed over the past 5 decades, depending on the region. As shown in Fig. 2, despite the increase in the regional number of power plants, the shift towards cleaner fuels in historically industri-

alised regions (such as Europe and North America), together with increased energy efficiency, has led to stable and lower CO₂ emissions in these regions (e.g. a 13 % decrease in emissions in Europe between 1970 and 2022). In contrast, emerging regions are characterised by significantly higher emissions in 2022 and the use of high-carbon-content fuels, such as coal. Over the past 5 decades, fossil CO₂ emissions from power plants have increased up to 42 and 38 times in China and India, respectively. Country-specific trends in CO₂ and GHG emissions from power plants are presented in Crippa et al. (2023c).

3.2 Industrial facilities and other point sources

Industrial activities cover a wide range of sectors, encompassing not only the production of iron and steel, cement, glass, metals, chemicals, and fertilisers and the use of solvents, but also intensive animal farming (see Sect. 3.4). Gathering information on industrial activities (e.g. production, capacity, and location of the facilities) at the global level is challenging, in part because of confidentiality and data protection issues. For this reason, we focused on not only the updating of information on industrial point sources (when available), but also improving the gap-filling method for all industrial activities if data are incomplete or missing (as discussed in detail in Sect. 3.5). In EDGAR v8.0, we included the latest E-PRTR (E-PRTR v18) locations for all industrial facilities (with the exception of power plants, iron and steel facilities, and coal mines, for which dedicated spatial proxies have been developed at the global level). Several manual adjustments were made to overcome data quality issues related to missing spatial information and inconsistencies. The analysis of the E-PRTR dataset also inspired the idea of attributing only a fraction of the emissions to the reported point sources. This is justified by the fact that industrial facilities have to report their emissions only if they fall above a certain threshold. The fraction of the emissions to be allocated to the available point sources is determined through the ratio between the E-PRTR emissions (typically of CO₂) and the corresponding EDGAR emissions. When the ratio is 1, all emissions are allocated to the point sources; when the ratio is lower than 1, the complementary fraction is then attributed to the gap-filling grid (i.e. non-residential proxy as defined in Sect. 3.5).

In EDGAR v8.0, we have also updated the global locations of iron and steel plants, which are among the most energy-intensive industries. The Global Steel Plant Tracker of the Global Energy Monitor (2022d) was used as a data source because of its global and temporal completeness (1970 to present). The installed capacity was used to weight the relative contribution of each iron and steel plant although it may represent an approximation of the real capacity in use. A map of iron and steel production plants in 1970 and 2022 is presented in Fig. 3. The number of iron and steel plants increased around 10-fold over the last 5 decades (from 77 to

728), with the sharpest increases in China (5-fold) and the United States and India (2.7-fold).

Coal mines are also a relevant source of fugitive emissions of GHGs and air pollutants (e.g. volatile organic compounds). In EDGAR v8.0, we updated the information on coal mines at the global level using the Global Coal Mine Tracker of the Global Energy Monitor (2022a) complemented by the EIA data for the United States (US EIA, 2022a). For countries not covered by these data sources, we relied on the previous EDGAR spatial proxies including data from the United States Geological Survey (USGS, 2019). More specifically, we included information on surface and underground mines for both hard and brown coal.

3.3 Venting and flaring

Gas flaring is the burning of the natural gas that results from oil extraction. Although this practice is highly polluting and represents a waste of resources, it still takes place in several countries because of economic constraints and a lack of appropriate legislation. Flaring takes place at both onshore and offshore installations, and it is a source of GHG and air pollutant emissions.

Global CO₂ emissions related to flaring accounted for 276 Mt in 2022, of which 76 % was emitted by 10 countries, namely Russia (18 % of the global total), Iraq (13 %), Iran (12 %), and Venezuela (7 %), followed by Algeria, United States, Mexico, Libya, Nigeria, and China. Although this emission source represents only 0.8 % of global CO₂ emissions, it is particularly relevant for certain regions of the world, such as Venezuela (20 % of the country's total CO₂ emissions), Iraq (18 %), Libya (17 %), Algeria (10 %), and Nigeria (9 %). Considering the relevance of venting emissions and the potential for control measures, it is essential to accurately quantify this source and attribute it to the correct location. Flaring emissions can also be localised and quantified using spaceborne measurements (Elvidge et al., 2017; NOAA, 2017). In EDGAR v8.0, data from the World Bank Global Gas Flaring Tracker Report (2023) were used for estimating both the emissions and the location of global flaring activities from 2012 to 2022. These spatial data were also used as a best approximation to spatially distribute emissions from venting, which is the controlled release of natural gas without it being burned, although the two activities may not overlap. The resulting map of CO₂ emissions in 2012 and 2022 is shown in Fig. 4.

3.4 Intensive livestock and fertiliser-manufacturing industries

Agriculture includes a variety of activities that are typically distributed over large areas (e.g. crop areas and animal pastures). However, several agricultural activities can be defined as hotspots or point sources and include intensive animal farming and manure management practices. In a broader

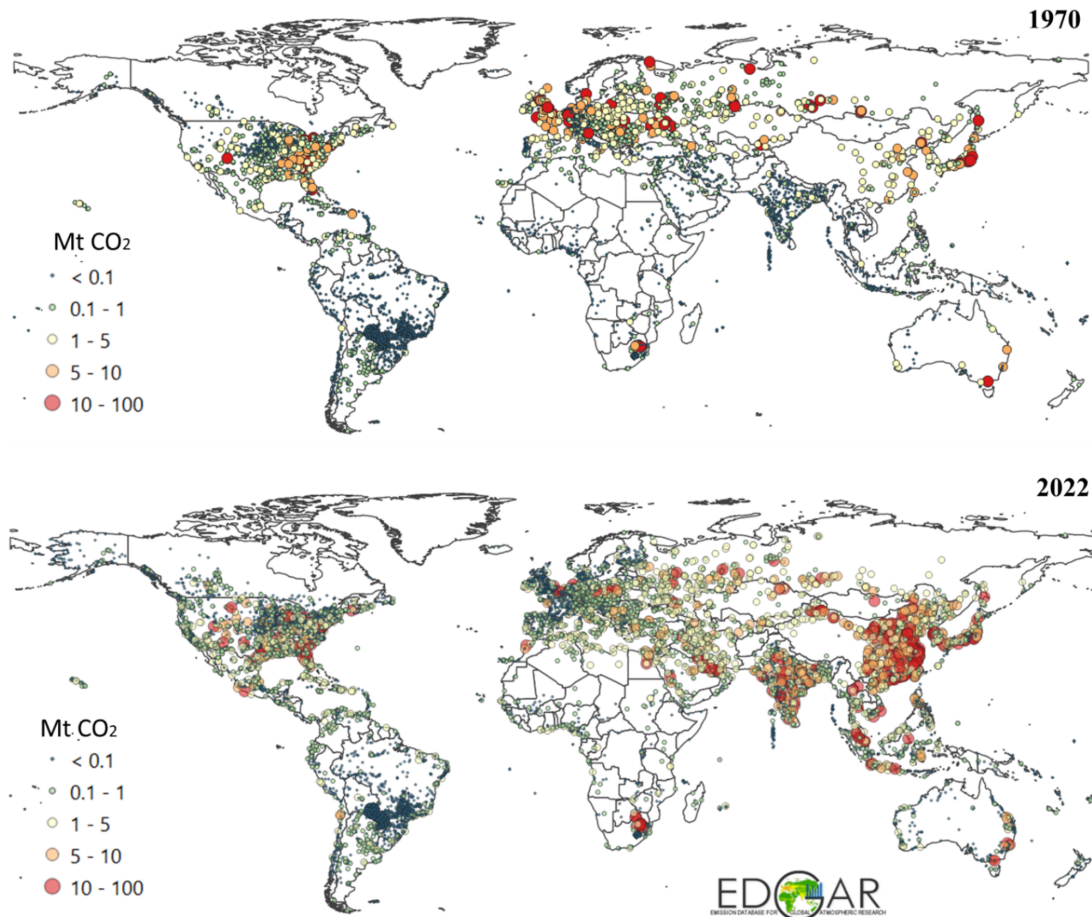


Figure 1. CO₂ emissions from fossil-fuel-fired power plants in 1970 and 2022 from EDGAR v8.0. The size of the circles is proportional to the magnitude of the emissions.

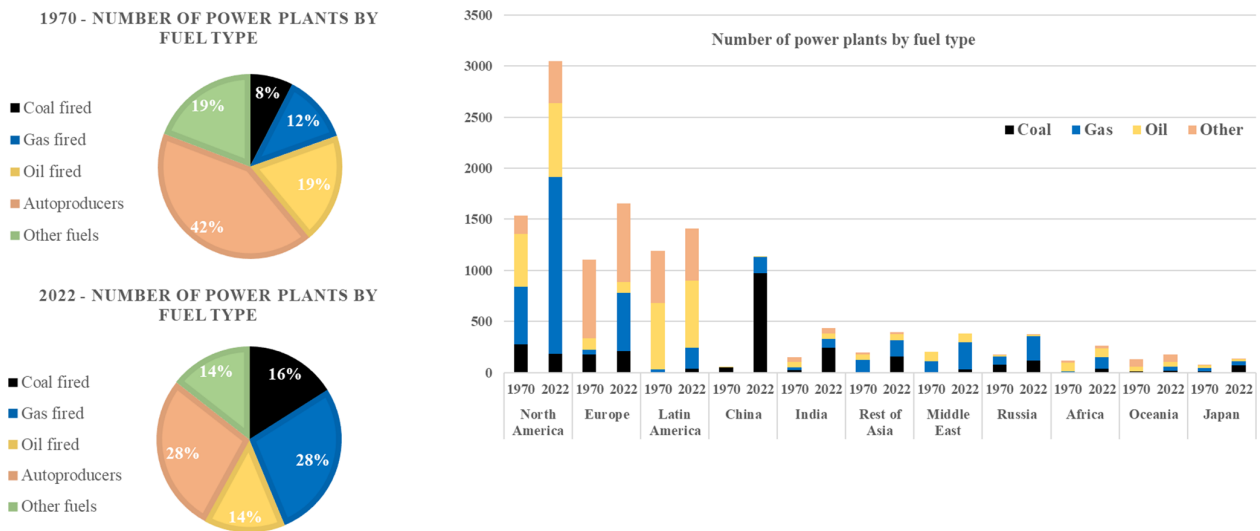


Figure 2. Increase in the total number of power plants (including fossil-fuel-fired and biofuel-fired plants) from 1970 to 2022 by world region, as included in the updated EDGAR spatial proxies.

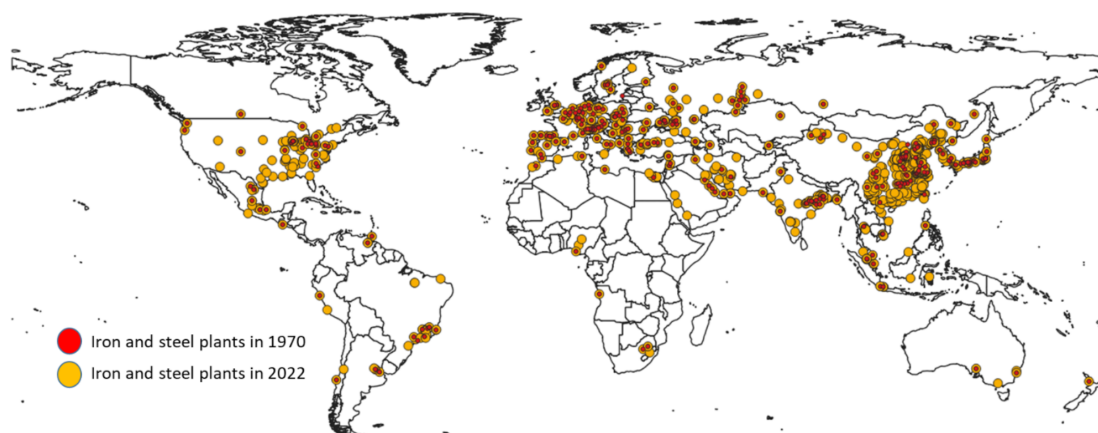


Figure 3. Global locations of iron and steel plants in 1970 and 2022.

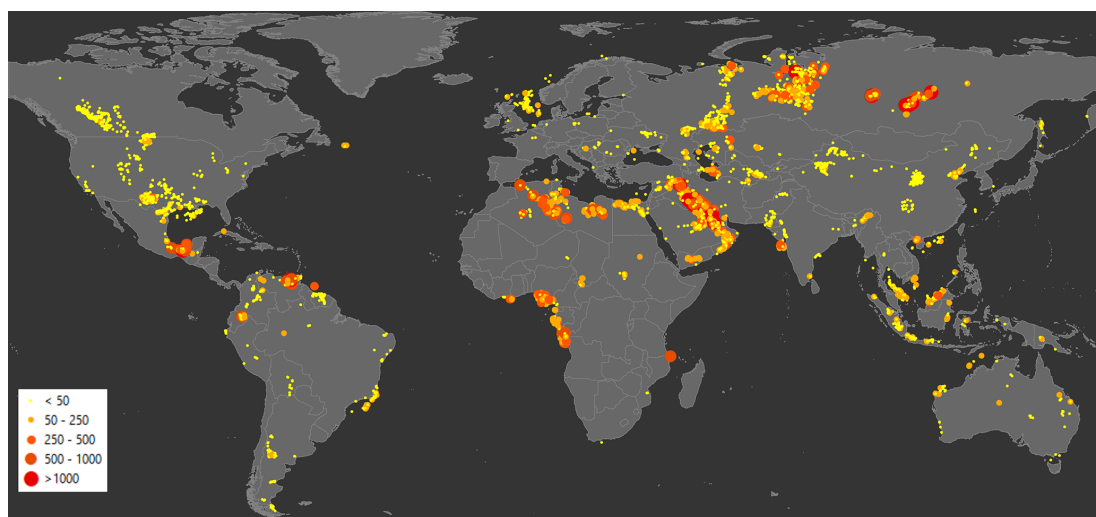


Figure 4. Global map of CO₂ emissions (in kt) from flaring in 2022.

sense, we also allocate the fertiliser-manufacturing industry to this sector, which represents an important source of NH₃ and N₂O. In EDGAR v8.0, the infrared atmospheric sounding interferometer (IASI) satellite-derived NH₃ point source database (Van Damme et al., 2018; Clarisse et al., 2019) is included to map emissions from animal farming and fertiliser production with yearly information for the period 2008–2022. It includes 270 agricultural hotspots and 251 synthetic NH₃ production facilities worldwide. Since the NH₃ point source database includes only hotspots, we decided to allocate only a fraction of the total emissions for that sector and country derived from approximate estimates of NH₃ emission fluxes from IASI measurements to these points, while distributing the remaining fraction to livestock density maps formerly available in EDGAR. Similarly to what was done for other industries, for Europe, intensive livestock and fertiliser production point sources were taken from E-PRTR v18. Similarly, the satellite-based information on fertiliser

industries was integrated into the previous EDGAR proxy for this sector. This update represents a significant improvement in representing nitrogen-related hotspots (Van Damme et al., 2018) compared with earlier EDGAR releases, which mostly used animal density as a proxy (see Table S1), albeit taking into account that the uncertainty in IASI information is around 50 %. A snapshot of N₂O emissions from manure management at the global level and in Europe, where intensive livestock activities appear as emission hotspots, is shown in Fig. 5.

3.5 Gap-filling missing information for point sources

A significant improvement is represented by the development and use of a new spatial proxy to gap-fill missing information for all industry-related emissions. Until EDGAR v7.0, population-related proxies were used as backup information when no spatial data were available to represent the emis-

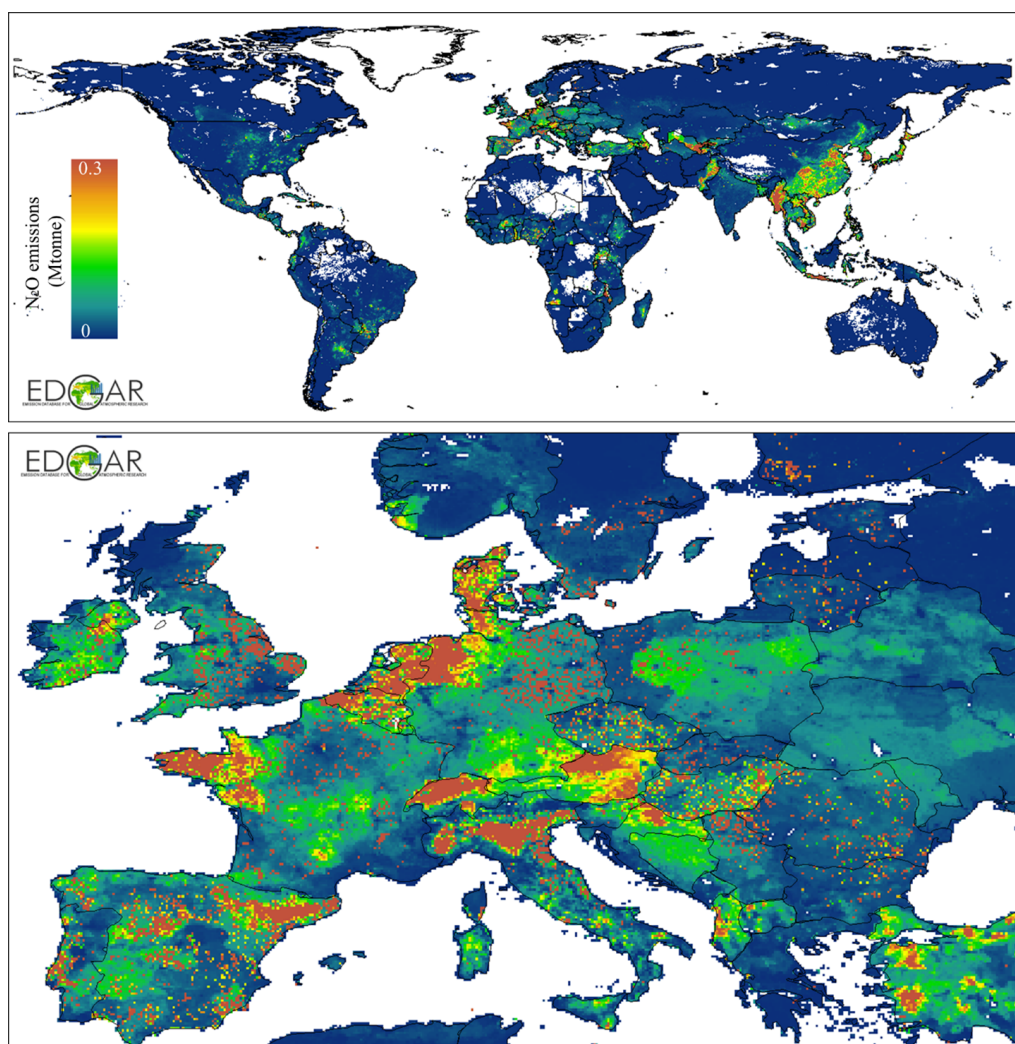


Figure 5. N_2O emissions from manure management at the global level and in Europe, where intensive livestock activities appear as emission hotspots.

sions for a sector within a country (Crippa et al., 2021). However, here we decided to use the non-residential built-up surface information developed by the GHSL (Pesaresi and Politis, 2023; European Commission, 2023) as a backup proxy to distribute the emissions of all the activities not related to small-scale combustion, for which no point source information was available (even for individual countries). This methodological assumption is a key novelty of this work because of its application at the global level. However, it is in line with methodologies already applied in regional inventories, such as in Europe (Kuenen et al., 2022), where the CORINE Land Cover dataset is used to spatially allocate emissions to areas with industrial activity, thus supporting the validity of this assumption.

For certain sectors and regions, this non-residential gap-filling proxy is also used to allocate a fraction of the emissions of certain sectors (see, for example, the industrial facil-

ities section for Europe). The overall effect of using this new proxy is a change in the industrial contribution over densely populated areas, which was previously higher in EDGAR than in other inventories for Europe in particular (Thunis et al., 2024). Figure 6 shows CO_2 emission maps from manufacturing industries obtained from EDGAR v7.0 and v8.0. This figure highlights the implications of using different gap-filling proxies for the industrial sector and in particular contrasts those based on population (EDGAR v7.0) with the new ones based on non-residential built-up surface data (EDGAR v8.0).

Overall, using non-residential built-up information to allocate emissions of industrial activities to complement point source information leads to lower emission levels being allocated to urban areas and a less densely distributed map over certain regions (e.g. China and India). Figure S3 shows the impact of this update on global fossil-fuel-derived CO_2 emis-

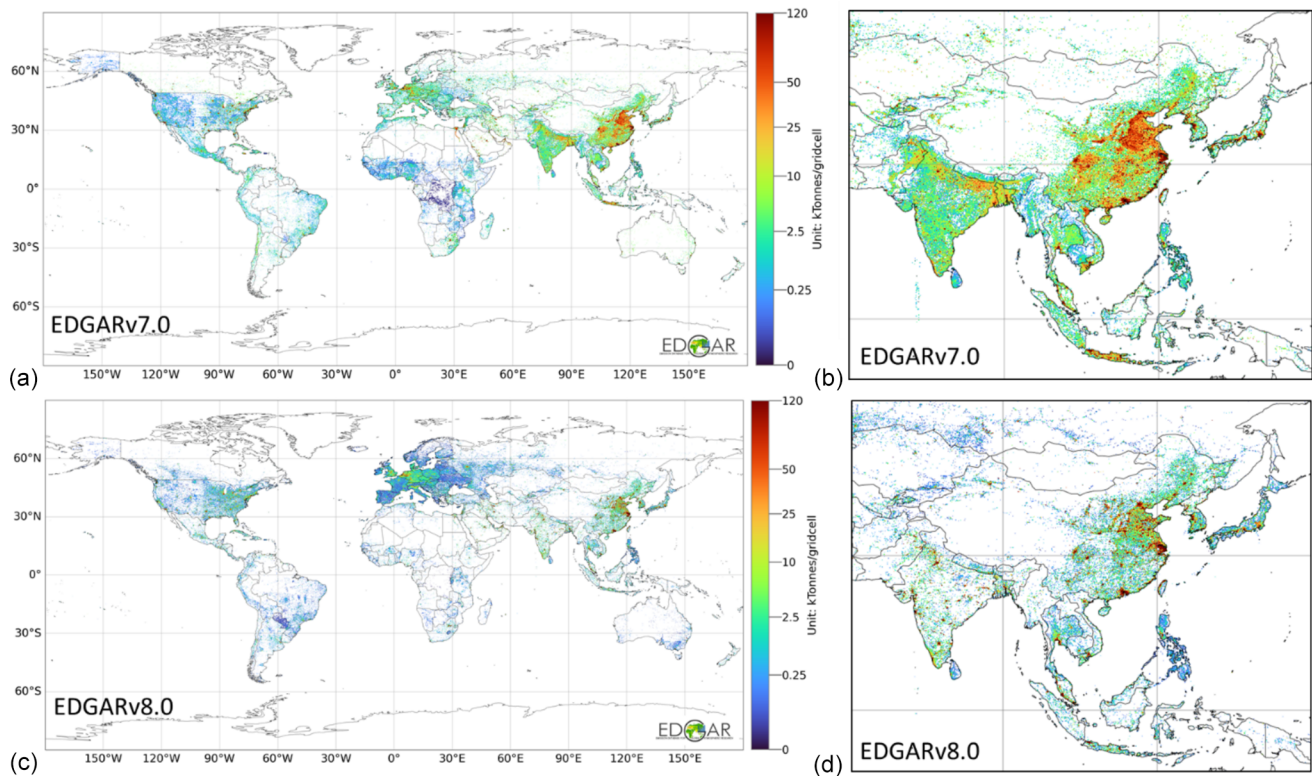


Figure 6. CO₂ emissions from industrial combustion in 2021 from EDGAR v7.0 (a, b) and v8.0 (c, d), showing the impact of the gap-filling proxies used for industrial sources.

sions from the industrial sector over global functional urban areas (FUAs) in 2022. The share of CO₂ industrial emissions in the national total over FUAs is typically higher, on average by around 30 %, in EDGAR v8.0 than in EDGAR v7.0 for several developing countries (e.g. Africa, India, and South America) because of the presence of industrial point sources and non-residential activities still close to urban areas. However, lower emissions from industries (on average around 20 % lower) are found in many industrialised regions (e.g. Europe, Oceania, and United States) because of the displacement of industrial activities in remote areas or outside the FUAs. This result represents the effect of using non-population-based proxies for industrial emissions in EDGAR v8.0 compared with previous EDGAR proxies.

4 Linear sources of emissions: international shipping

Since EDGAR v6.0, international shipping emissions have been distributed using the Ship Traffic Emission Assessment Model (STEAM3) from the Finnish Meteorological Institute (Jalkanen et al., 2012; Johansson et al., 2017) and this approach has remained unchanged in EDGAR v8.0. Emissions are distributed on a yearly basis from 2000 to 2018, including multi-vessel information (cargo, container, fishing, passenger

cruiser, service, tanker, vehicle carrier, and miscellaneous). Compared with the previous EDGAR proxy, the use of the STEAM data allows for a better representation of the trend over time in international shipping emissions, differentiating the variation in the routes and their intensity for the different vessels on an annual basis consistently with the information available in EDGAR (see Fig. 7). Only data covering sea areas are included since inland data over big rivers or lakes are not robust enough to be included in EDGAR. Information on emission control areas and in particular on sulfur and NO_x emission control areas is not included yet, although this may be considered in future updates of EDGAR. A comparison between the international shipping intensities available in EDGAR before and after this update is presented in Fig. S4 of the Supplement.

Figure 8 focuses on three main vessel types representing the largest fraction of GHG emissions from international shipping in 2022 and contributing specifically around 22 % (tankers), 24 % (containers), and 28 % (cargo) of total international shipping GHG emissions. The impact of using the STEAM data to develop the new spatial proxies for international shipping is shown in Fig. 8, which presents a comparison between EDGAR v5.0 and EDGAR v8.0 CO₂ emissions from the three main vessel types over the different oceans and seas. EDGAR v5.0 used an in-house EDGAR

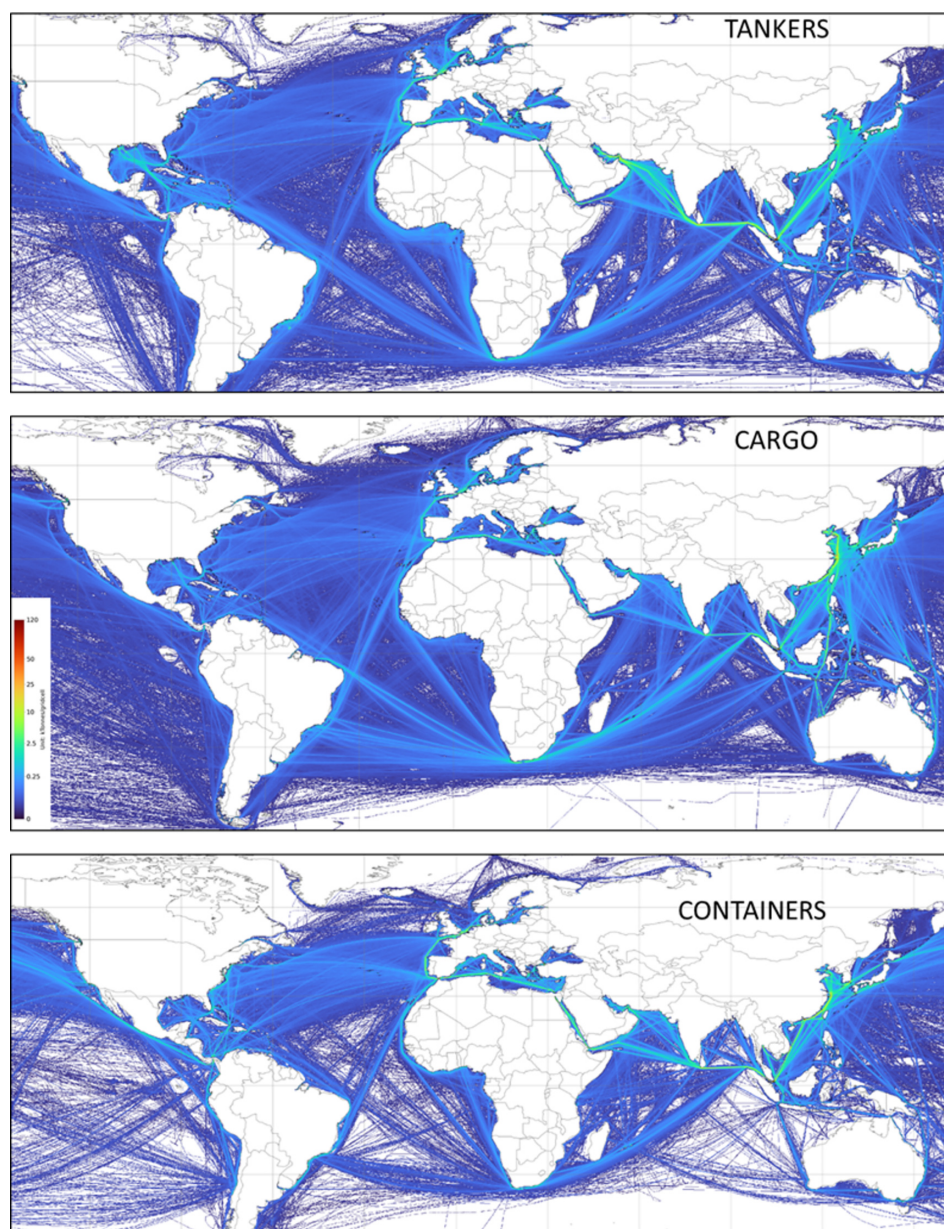


Figure 7. International shipping GHG emissions in 2021 showing the ship tracks for tankers, cargo vessels, and containers as in EDGAR v8.0.

proxy based on Wang et al. (2008), improved with long-range identification and tracking information (Alessandrini et al., 2017) for European seas, as described in Janssens-Maenhout et al. (2019). EDGAR v5.0 proxies allocated most of the international shipping emissions over the Atlantic and Pacific oceans, while the new proxies for EDGAR v8.0 allocate the largest portion of these emissions (40 %) over the seas around China, Japan, and the Philippines. There is also a major difference in the relative share of tanker emissions over the Mediterranean Sea between the two versions, with the largest contribution (85 %) from the three categories being considered in EDGAR v5.0. Emissions allocated to the Gulf

of Mexico and Arabian Sea are 2 times higher when using the STEAM-based proxies in EDGAR v8.0.

5 Area sources of emissions

5.1 Residential activities

Small-scale combustion emissions are mostly related to non-industrial activities, such as those from the residential, commercial, agricultural, and fishing sectors. Therefore, population-based spatial proxies are often used to downscale national emissions. EDGAR v8.0 aims to couple popula-

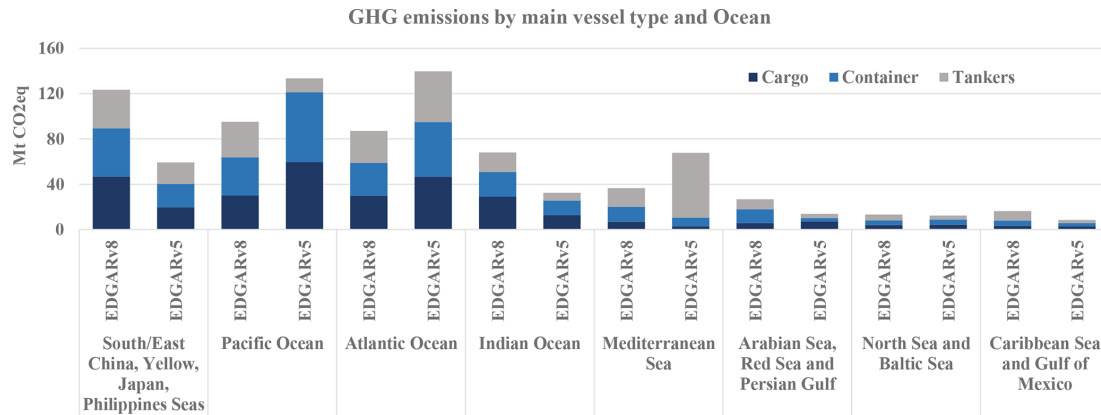


Figure 8. Comparison between GHG emissions from international shipping in 2022 by main vessel type and ocean or sea from EDGAR v5.0 and v8.0. Fishing-, service-, and passenger-related emissions are excluded from this comparison.

tion distribution with heating degree-days (HDDs) since the amount of emissions is dependent on not only the number of people living in a certain area, but also the meteorological conditions and the need for heating indoor spaces. Residential emissions are therefore distributed considering both population intensities and heating needs, with varying profiles from 1970 to 2022. EDGAR v8.0 includes the latest population grid maps developed by Global Human Settlement, GHS-POP R2023A (Schiavina et al., 2023b; Freire et al., 2016), which comprise residential population information for 12 epochs, over 1975–2020, with 5-year time steps, and projections to 2025 and 2030 obtained by distributing census data from CIESIN GPWv4.11 over global grid maps. GHS-POP R2023A data at 30 arcsec (WGS84, EPSG:4326) (or about 1 km) spatial resolution were used to develop the corresponding spatial proxies in EDGAR. Population density is then calculated for each grid cell and used as a proxy to allocate household emissions over populated areas. Small-scale combustion activities related to agriculture are distributed using rural population maps obtained from the GHS-SMOD R2023A product (including only low-density and very-low-density rural grid cells) (Schiavina et al., 2023a). For missing years, the closest population map to each epoch is taken (e.g. for the years 2001 and 2002, the population map from 2000 is used, while for the years 2003 and 2004, the 2005 map is used).

To account for the effect of the weather (ambient temperature) on heating needs in the residential sector, heating degree-days (HDDs) were computed using the 2 m surface air temperature data with an hourly time resolution and $1^\circ \times 1^\circ$ spatial resolution using the Copernicus ERA5 atmospheric reanalysis produced by the European Centre for Medium-Range Weather Forecasts for the years 1970–2022 (https://cds.climate.copernicus.eu/cdsapp#!/dataset/reanalysis-era5-single-levels?tab=_form, last access: November 2023). HDDs are the cumulative number of degrees by which the mean daily temperature falls below a

reference temperature (usually 18°C or 19°C , which is adequate for human comfort). HDDs were calculated following the methodology described by Spinoni et al. (2018) and assuming a reference temperature of 18°C . Cooling degree-days are not included in the development of the spatial proxies since they are mainly related to electricity consumption rather than to fuel combustion in the residential sector. An additional weight is therefore added to the population distribution using the HDD metric, thus increasing the emissions arising in colder regions with a greater need for heating than in warm areas for the same amount of population.

Our approach does not aim to identify and represent heating habits for all countries but modulates the differences in combustion of fuels within a single country for heating purposes due to the different mean temperatures across latitudes (climatic zones). Country populations may also have different habits in terms of turning on and off their heating systems, thus requiring the use of different reference temperature values in the calculation of HDDs (Atalla et al., 2018), which is not taken into account here. The process of building the residential proxy in EDGAR is shown in Fig. 9.

6 Results

The purpose of this work was to describe the methodological improvements included in EDGAR v8.0 linked to the update of the spatial data used to downscale country-specific and sector-specific emissions. In addition, a specific focus is dedicated to case studies showing the relevance of understanding the trends in GHG emissions at the subnational level in order to support the development of regional climate mitigation and adaptation policies (Kuramochi et al., 2020). The reader can refer to Crippa et al. (2023c) for a description of country-specific and sector-specific GHG emission trends at the global level. In the following sections, insights into the global distribution of GHG emissions and their subnational features are described.

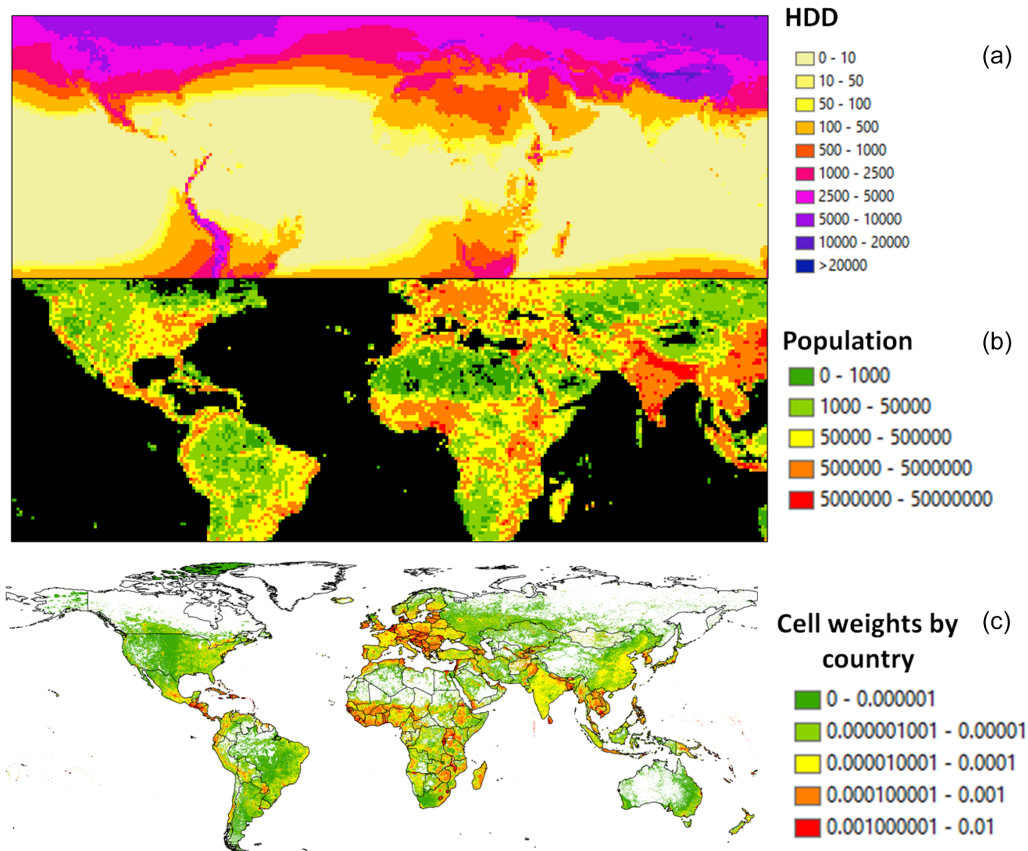


Figure 9. Coupling HDDs (a) with population density, (b) as a proxy, and (c) to downscale residential emissions. Data are for the year 2020.

6.1 Global greenhouse gas emissions in EDGAR v8.0

Figure 10 shows global GHG emissions in 2022 as a result of the EDGAR v8.0 gridding process, while Fig. 11 reports the same emissions at the country and subnational levels. Complementary figures are also presented in the Supplement. The maps in Figs. S5–S8 show the trends in global emissions of GHGs and fossil-fuel-derived CO₂, CH₄, and N₂O from 1970 to 2022.

The main strength and novelty of EDGAR v8.0 is related to the production of a global GHG emission database at different levels of granularity to support local, regional, and global climate actions. The high-spatial-resolution global maps are available at a 0.1° × 0.1° resolution WGS84 (EPSG:4326), equalling about a 10 km spatial resolution at the Equator, as both emissions and emission fluxes (.txt and .NetCDF files; https://edgar.jrc.ec.europa.eu/dataset_ghg80, last access: June 2024). They not only fulfil the requirements of the global atmospheric modelling community, but also bridge bottom-up and top-down (mostly satellite-based) GHG emission estimates (see Fig. 10).

EDGAR v8.0 allows for full flexibility in the aggregation of emissions at the subnational level, thus supporting the analysis of the spatio-temporal variability in the emissions at the grid-cell level and over wider administrative

domains or areas of interest such as urban centres (Melchiorri, 2022). A second key product from EDGAR v8.0 is represented by GHG emissions at the subnational level using the Global ADMINISTRATIVE layer version 4.1 (https://gadm.org/download_country.html, last access: June 2024) at level 1 and the NUTS 2 level for the EU extended geographical domain, as shown in Fig. 11.

Looking at province-scale or city-scale emissions requires not only associating, for example, point sources to the NUTS 3 level, but also relying on an approach different from the downscaling of national totals, which may include the use of statistical information available over smaller territorial units. Therefore, considering the current purposes of EDGAR, the NUTS 2 level represents the right balance between the accuracy of the final emission data and downscaling of national totals. The relevance of including country-specific details and subregional information is essential when doing emission data extraction at the subnational level, thus avoiding border issues. Some inventory compilers (Kuenen et al., 2022) report point source information as just points, without distributing them over a grid map with a certain resolution. This approach is accurate since it provides the exact geographical coordinates of individual facilities; however, it does not reduce data extraction issues since the allocation of

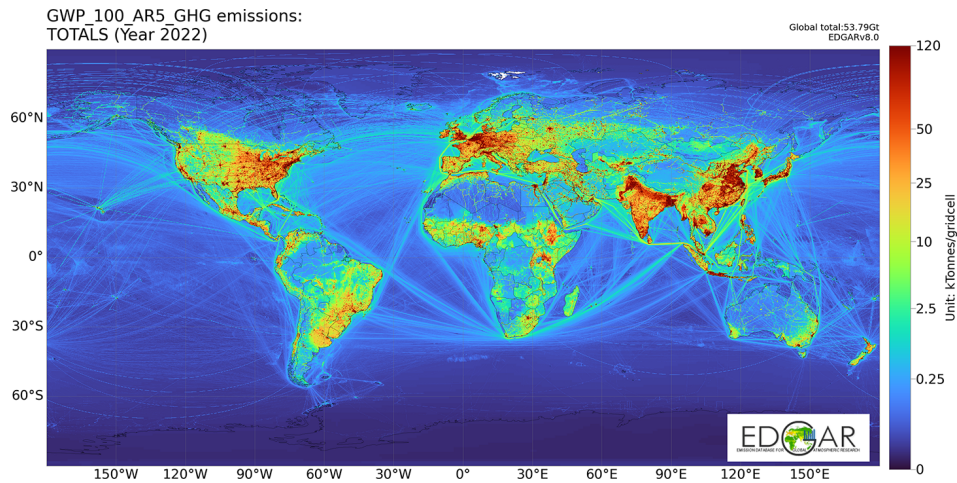


Figure 10. Global GHG (expressed in kt CO₂ equivalent) emission map in 2022 from EDGAR v8.0.

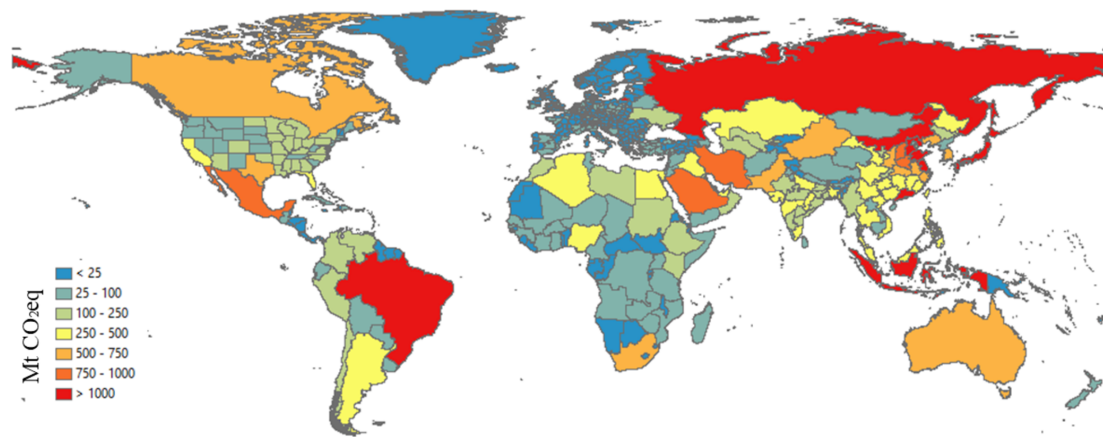


Figure 11. Global GHG emissions at the national and subnational levels in 2022 from EDGAR v8.0.

a specific point to a certain grid cell may fall at the border of, for example, two or more regions.

Another challenge that we address with this new gridding approach is related to the harmonisation of national and subnational data. Local and regional inventories are often developed independently, thereby undermining the possibility of combining subnational emission data to retrieve the national values. The challenge of using different and unharmonised databases is overcome by the EDGAR database as users are able to work consistently at both the national and regional levels, thus offering them the possibility of working across different geographical scales. This is achieved through the downscaling of national emission data to subnational data, making use of high-spatial-resolution proxies, as discussed in this paper. In Sect. 6.2 and 6.3, case studies in the European, American, and Asian domains are discussed more in detail.

6.2 Subnational emissions: the EU case

Climate and environmental territorial policies require robust and consistent knowledge of GHG and air pollutant emissions at the subnational level (e.g. NUTS 2). No subnational official reporting is available, and the high-spatial-resolution data available from EDGAR fill this knowledge gap. EDGAR subnational GHG emissions are used as a reference by the European Commission in cohesion reports (European Union, 2022, 2024), the European semester process and climate action territorial analysis. Figure 12 shows how GHG emissions at the NUTS 2 level changed between 1990 and 2021 in absolute, per capita, and per gross domestic product term. Out of 242 EU regions, 155 regions have shown a downwards trend in emissions since 1990, and 206 and 204 regions have done so since 2005 ($-1.27\% \text{ yr}^{-1}$ on average) and 2010 ($-1.35\% \text{ yr}^{-1}$ on average), respectively. However, in 2021, only 34 regions achieved GHG emissions of less than 5 t CO₂ equivalent per person, which is the average value needed to achieve the 2030 EU climate targets. The

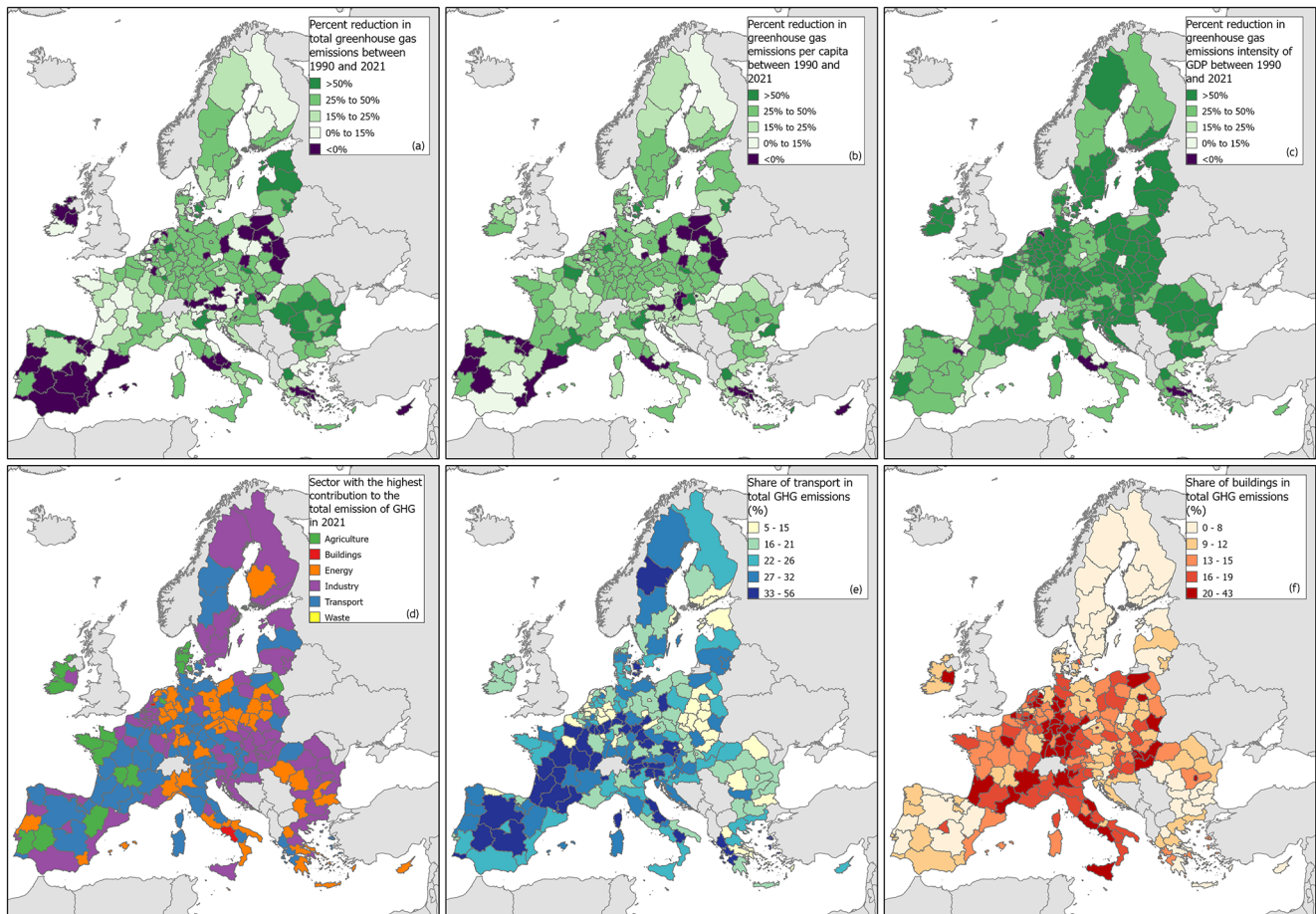


Figure 12. Relative change in EU GHG emissions by NUTS 2 level between 1990 and 2021 (a, b, c). Sectoral contribution to EU GHG emissions by NUTS 2 level in 2021 (d, e, f). The sector with the highest contribution in 2021 for each NUTS 2 region is shown in the map in the left panel. The contribution of GHG emissions from transport (e) and buildings (f) to total emissions in 2021 in the EU by NUTS 2 level is also shown.

sectors which contribute the most to total EU GHG emissions in 2021 are power generation (27 %), industry (23 %), transportation (20 %), buildings (14 %), and agriculture (11 %), showing that the different regions in the EU have different transition challenges. For example, when looking at the NUTS 2 level (see Fig. 12, bottom-middle panel), the transport sector is often the sector with the largest contribution at the regional level, in particular in rural regions of Spain, France, Italy, and Germany. Figure 12 (bottom-right panel) also shows the share of GHG emissions arising from small-scale combustion (buildings sector) at the NUTS 2 level, highlighting several regions for which this sector contributes more than 15 %–20 % to the regional total.

6.3 Subnational emissions in the United States, China, and India

EDGAR v8.0 also includes GHG emission estimates at the subnational level for the United States (i.e. estimates for each

US state; Fig. 13) and for each Chinese province and Indian state (Fig. 14). Based on our analysis, Texas emitted 11.5 % of the total US GHG emissions in 2022, followed by California with a contribution of 7.7 %, and Florida, with a share of 4.6 %. In 1990, Texas and California were the most-emitting states, followed by Ohio, Pennsylvania, and Illinois. Over the past 3 decades, the sector with the highest share of GHG emissions at the state level over the United States has changed, with a shift from power generation and industry towards transport (see Fig. 13).

In 2022, the five most-emitting Chinese provinces contributed around 40 % of China's total GHG emissions. These were Shandong (8.9 % of the country total), Guangdong (8.4 %), Jiangsu (7.4 %), Hebei (6.6 %), and Nei Mongol (6.5 %), findings consistent with other studies addressing provincial CO₂ and GHG emissions in China (Jiang et al., 2019; Zhang et al., 2020). In 1990, the top five emitting provinces were Shandong (8.1 %), Hebei (6.5 %), Jiangsu

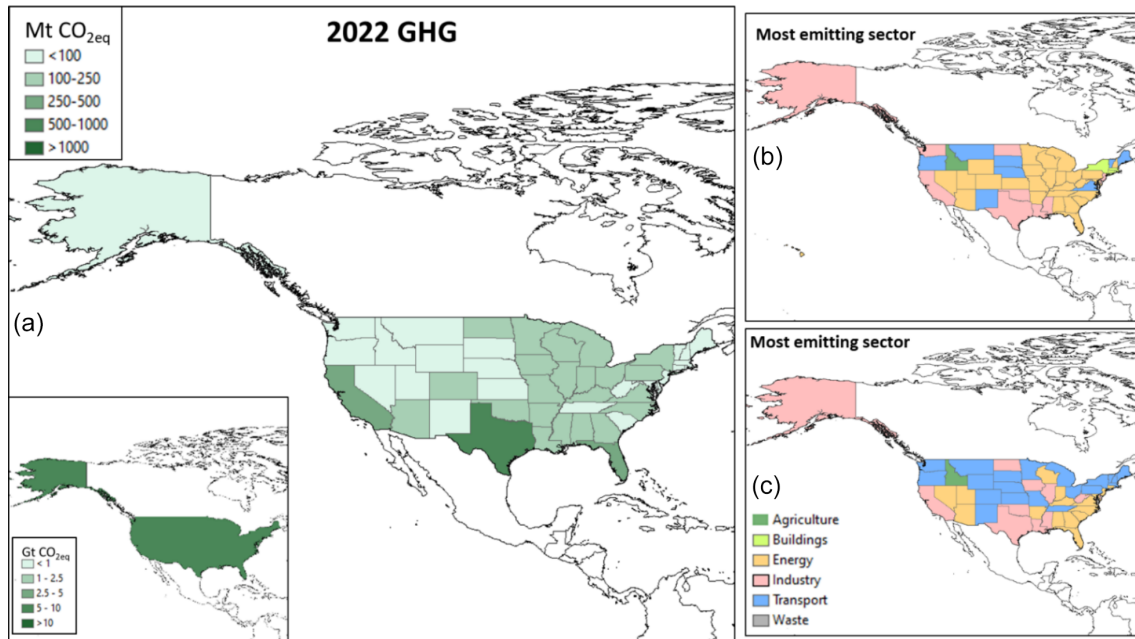


Figure 13. GHG emissions for 2022 at the subnational level in the United States (a) and the sector with the highest contribution to total emissions in 1990 and 2022 for each US state (b, c).

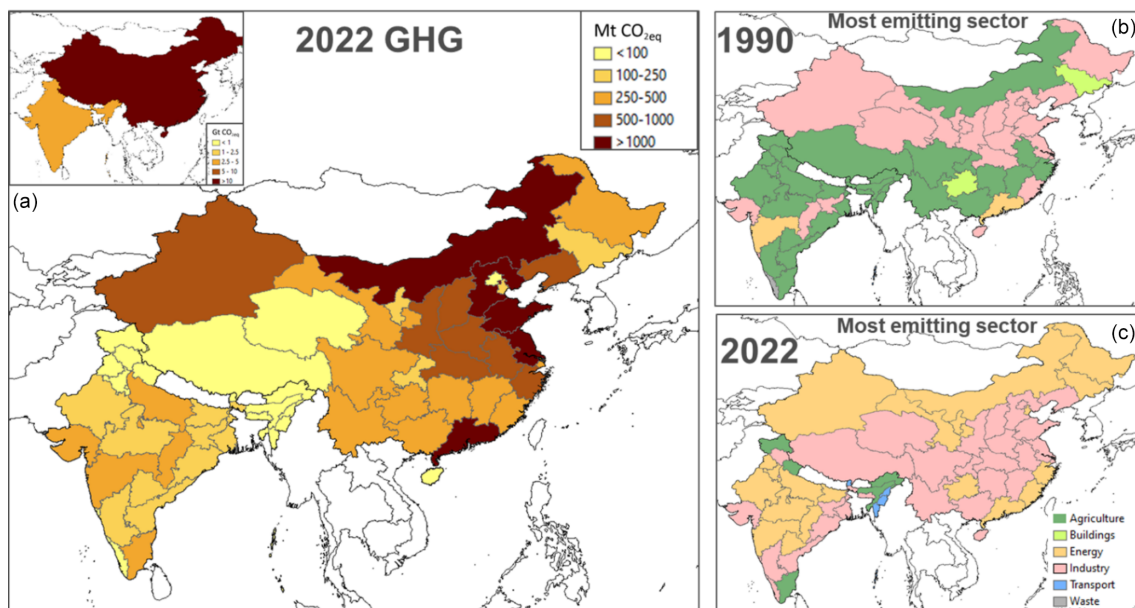


Figure 14. GHG emissions for 2022 at the subnational level over the Asian domain, with a focus on China and India (a) and the sector with the highest contribution in 1990 and 2022 for each Chinese province and Indian state (b, c).

(6.2 %), Henan (5.9 %), and Nei Mongol (5.8 %), contributing around 30 % to China's total GHG emissions.

In 2022, five Indian states contributed around 50 % of the country's total GHG emissions, namely Maharashtra (11.8 %), Tamil Nadu (11.7 %), Uttar Pradesh (8.1 %), Gujarat (8.0 %), and Chhattisgarh (6.6 %). In 1990, the most-emitting Indian states were Tamil Nadu (18.4 %), Maharash-

tra (9.5 %), Uttar Pradesh (9.3 %), West Bengal (6.6 %), and Andhra Pradesh (6.0 %). Compared with the US and European cases, the picture is different over the Asian domain in terms of the top-emitting sectors at the subnational level (Fig. 14). The effect of India's economic growth and its transition from an agricultural economy to a more industrialised economy can be seen in Fig. 14 (right panels). As a result,

the sectors with the highest share of GHG emissions changed from agriculture (in 1990) to energy and industry (in 2022) over China and India, with the exception of a few regions (e.g. Tamil Nadu, Assam, Jammu and Kashmir, and Uttarakhand) that still had an agriculture-based economy in 2022. This type of information and analysis is instrumental for the definition of effective sector-specific climate change mitigation actions at the subnational level.

7 Data availability

The EDGAR v8.0 GHG global emission maps can be freely accessed at <https://doi.org/10.2905/b54d8149-2864-4fb9-96b9-5fd3a020c224> (Crippa et al., 2023a). The EDGAR v8.0 subnational emissions can be accessed at <https://doi.org/10.2905/D67EEDA8-C03E-4421-95D0-0ADC460B9658> (Crippa et al., 2023b). All data can also be accessed through the EDGAR website at https://edgar.jrc.ec.europa.eu/dataset_ghg80 and https://edgar.jrc.ec.europa.eu/dataset_ghg80_nuts2 (last access: June 2024).

Data are made available as emission grid maps for each species and for total GHGs as .txt and .nc files with emissions expressed in tonnes of substance per $0.1^\circ \times 0.1^\circ \text{ yr}^{-1}$. Emission fluxes are available as .nc files and they are expressed in kilograms of substance $\text{m}^{-2} \text{ s}^{-1}$. Emission maps are available as both total and sector-specific emissions.

8 Conclusions

Climate targets are often set at the global and national levels; however, their implementation may occur at the subnational level. It is therefore of utmost relevance to develop subnational GHG emission estimates for policy development, to monitor progress towards climate targets, or to evaluate their impacts.

This work summarises the main updates to EDGAR concerning the use of high-resolution and up-to-date spatial information to improve the global geospatial disaggregation of GHG emissions at the subnational level. Having accurate and up-to-date sector-specific global maps of GHG emissions at high spatial resolution ($0.1^\circ \times 0.1^\circ$) is instrumental for the design of effective climate change mitigation options beyond (inter)national climate targets. EDGAR v8.0 spatial proxies include globally consistent spatial data derived, for example, from the Global Energy Monitor, the GHSL work, satellite-based information for computing HDDs or for identifying hotspots from agricultural activities, STEAM for ship tracking, and many other global datasets. The use of satellite data to improve the EDGAR spatial proxies represents a successful cooperation between bottom-up inventory compilers and the Earth observation community and the potential to integrate relevant satellite-based datasets and statistical informa-

tion. In addition, EDGAR v8.0 integrates spatial information from local databases (e.g. E-PRTR for Europe and EIA data for the United States) when including data more detailed than those available in global databases.

Continuous updates and improvements in the spatial data used to downscale national emissions over the global grid are required to accurately represent trends in emission sources and their location. The strength and uniqueness of the EDGAR work arises from its global coverage and consistency in computing and representing emissions for all countries, and it has thus become a reference for many countries with limited capabilities for estimating their emissions. However, several challenges are associated with the use of global databases, in particular when dealing with the collection of point sources. Therefore, the use of local data, if available, is recommended when performing analysis at the highest spatial resolution (e.g. at the city level).

A further improvement in EDGAR is related to the inclusion of subnational information, representing a unique feature that can address the evaluation of spatial patterns in trends in subnational GHG emissions in a consistent way. Such a spatial resolution and subnational sector-specific variability prepare the ground for the production of city-level emission data records, as used, for example, in the Urban Centre Database (Melchiorri et al., 2024). In this paper, a few case studies are presented, with the main focus being on the European case, where the EDGAR subnational data are regularly used as input to the European semesters and contribute to climate action territorial and cohesion policies through the EU cohesion reports.

The EDGAR v8.0 data release provides an improved GHG dataset that could be useful not only for air quality modellers, but also for policymakers willing to analyse subnational GHG emission patterns. Future EDGAR activities will focus on delivering an updated dataset for air pollutants, including the latest spatial information made available through this work.

Supplement. The supplement related to this article is available online at: <https://doi.org/10.5194/essd-16-2811-2024-supplement>.

Author contributions. MC, DG, and FP have designed and developed the work on the update of the spatial proxies in EDGAR. MS, MM, and LD have developed the GHSL products used as input for this work. FG processed the Copernicus temperature data to produce HDD data. MM, EP, and JM contributed to the data analysis of the EDGAR emission maps. MVD, LC, and PC developed the IASI measurements and performed corresponding data processing and analysis. All co-authors contributed to the drafting of the paper.

Competing interests. The contact author has declared that none of the authors has any competing interests.

Disclaimer. The views expressed in this publication are those of the authors and do not necessarily reflect the views or policies of the European Commission.

Publisher's note: Copernicus Publications remains neutral with regard to jurisdictional claims made in the text, published maps, institutional affiliations, or any other geographical representation in this paper. While Copernicus Publications makes every effort to include appropriate place names, the final responsibility lies with the authors.

Acknowledgements. We are grateful to William Becker for the thorough review and proofreading of this paper. All emissions, except CO₂ emissions from fuel combustion, are from the EDGAR community GHG database comprising IEA-EDGAR CO₂, EDGAR CH₄, EDGAR N₂O, and EDGAR F-gases version 8.0 (2023). The IASI-NH₃ catalogue was updated in the framework of the European Space Agency World Emission project (<https://www.world-emission.com>, last Access: June 2024). The Université Libre de Bruxelles also gratefully acknowledges support from the TAPIR project (Air Liquide Foundation).

Financial support. This research was supported by the Directorate-General for Regional and Urban Policy of the European Commission (DG REGIO; JRC administrative agreement no. 36325; grant no. 2022CE160AT124).

Review statement. This paper was edited by David Carlson and reviewed by two anonymous referees.

References

- Ahsan, H., Wang, H., Wu, J., Wu, M., Smith, S. J., Bauer, S., Suchyta, H., Olivié, D., Myhre, G., Matsui, H., Bian, H., Lamarque, J.-F., Carslaw, K., Horowitz, L., Regayre, L., Chin, M., Schulz, M., Skeie, R. B., Takemura, T., and Naik, V.: The Emissions Model Intercomparison Project (Emissions-MIP): quantifying model sensitivity to emission characteristics, *Atmos. Chem. Phys.*, 23, 14779–14799, <https://doi.org/10.5194/acp-23-14779-2023>, 2023.
- Alessandrini, A., Guizzardi, D., Janssens-Maenhout, G., Pisoni, E., Trombetti, M., and Vespe, M.: Estimation of shipping emissions using vessel Long Range Identification and Tracking data, *J. Maps*, 13, 946–954, <https://doi.org/10.1080/17445647.2017.1411842>, 2017.
- Atalla, T., Gualdi, S., and Lanza, A.: A global degree days database for energy-related applications, *Energy*, 143, 1048–1055, <https://doi.org/10.1016/j.energy.2017.10.134>, 2018.
- Bieser, J., Aulinger, A., Matthias, V., Quante, M., and Denier van der Gon, H. A. C.: Vertical emission profiles for Europe based on plume rise calculations, *Environ. Pollut.*, 159, 2935–2946, <https://doi.org/10.1016/j.envpol.2011.04.030>, 2011.
- CEIP: Inventory Review 2021 Review of emission data reported under the LRTAP Convention, https://www.ceip.at/fileadmin/inhalte/ceip/00_pdf_other/2021/inventoryreport_2021.pdf (last access: August 2023), 2021.
- Clarisse, L., Van Damme, M., Clerbaux, C., and Coheur, P.-F.: Tracking down global NH₃ point sources with wind-adjusted superresolution, *Atmos. Meas. Tech.*, 12, 5457–5473, <https://doi.org/10.5194/amt-12-5457-2019>, 2019.
- Crippa, M., Guizzardi, D., Muntean, M., Schaaf, E., Dentener, F., van Aardenne, J. A., Monni, S., Doering, U., Olivier, J. G. J., Pagliari, V., and Janssens-Maenhout, G.: Gridded emissions of air pollutants for the period 1970–2012 within EDGAR v4.3.2, *Earth Syst. Sci. Data*, 10, 1987–2013, <https://doi.org/10.5194/essd-10-1987-2018>, 2018.
- Crippa, M., Guizzardi, D., Pisoni, E., Solazzo, E., Guion, A., Muntean, M., Florczyk, A., Schiavina, M., Melchiorri, M., and Hutfilter, A. F.: Global anthropogenic emissions in urban areas: patterns, trends, and challenges, *Environ. Res. Lett.*, 16, 074033, <https://doi.org/10.1088/1748-9326/ac00e2>, 2021.
- Crippa, M., Guizzardi, D., Pagani, F., Banja, M., Muntean, M., Schaaf, E., Becker, W., Monforti-Ferrario, F., Quadrelli, R., Riquez Martin, A., Taghavi-Moharamli, P., Grassi, G., Rossi, S., Brandao De Melo, J., Oom, D., Branco, A., San-Miguel, J., Vignati, E.: EDGAR v8.0 Greenhouse Gas Emissions, European Commission, Joint Research Centre (JRC) [data set] <https://doi.org/10.2905/b54d8149-2864-4fb9-96b9-5fd3a020c224>, 2023a.
- Crippa, M., Guizzardi, D., Pagani, F., and Pisoni, E.: GHG Emissions at sub-national level, European Commission, Joint Research Centre (JRC) [data set], <https://doi.org/10.2905/D67EEDA8-C03E-4421-95D0-0ADC460B9658>, 2023b.
- Crippa, M., Guizzardi, D., Pagani, F., Banja, M., Muntean, M., Schaaf, E., Becker, W., Monforti-Ferrario, F., Quadrelli, R., Riquez Martin, A., Taghavi-Moharamli, P., Köykkä, J., Grassi, G., Rossi, S., Brandao De Melo, J., Oom, D., Branco, A., San-Miguel, J., and Vignati, E.: GHG emissions of all world countries, Publications Office of the European Union, JRC134504, Luxembourg, <https://doi.org/10.2760/953322>, 2023c.
- de Meij, A., Krol, M., Dentener, F., Vignati, E., Cuvelier, C., and Thunis, P.: The sensitivity of aerosol in Europe to two different emission inventories and temporal distribution of emissions, *Atmos. Chem. Phys.*, 6, 4287–4309, <https://doi.org/10.5194/acp-6-4287-2006>, 2006.
- Elvidge, C. D., Baugh, K., Zhizhin, M., Hsu, F. C., and Ghosh, T.: Supporting international efforts for detecting illegal fishing and GAS flaring using viirs, 2017 IEEE International Geoscience and Remote Sensing Symposium (IGARSS), 23–28 July 2017, 2802–2805, <https://doi.org/10.1109/IGARSS.2017.8127580>, 2017.
- European Commission: GHSL Data Package 2023, Publications Office of the European Union, Luxembourg, JRC133256, <https://doi.org/10.2760/098587>, 2023.
- European Union: Cohesion in Europe towards 2050 – Eighth report on economic, social and territorial cohesion, edited by: Dijkstra, L., Publications Office of the European Union, <https://doi.org/10.2776/624081>, 2022.
- European Union: European Commission, Joint Research Centre (JRC), EDGAR (Emissions Database for Global Atmospheric Research) Community GHG database, comprising IEA-EDGAR CO₂, EDGAR CH₄, EDGAR N₂O and EDGAR F-gases

- version 8.0, https://edgar.jrc.ec.europa.eu/dataset_ghg80, <http://data.europa.eu/89h/b54d8149-2864-4fb9-96b9-5fd3a020c224> (last access: June 2024), 2023.
- European Union: Ninth Report on Economic, Social and Territorial Cohesion, Luxembourg, Publications Office of the European Union, ISBN 978-92-68-10894-9, <https://doi.org/10.2776/585966>, 2024.
- EUROSTAT: <https://ec.europa.eu/eurostat/web/gisco/geodata/reference-data/administrative-units-statistical-units/nuts> (last access: June 2024), 2021.
- Feng, L., Smith, S. J., Braun, C., Crippa, M., Gidden, M. J., Hoesly, R., Klimont, Z., van Marle, M., van den Berg, M., and van der Werf, G. R.: The generation of gridded emissions data for CMIP6, *Geosci. Model Dev.*, 13, 461–482, <https://doi.org/10.5194/gmd-13-461-2020>, 2020.
- Freire, S., MacManus, K., Pesaresi, M., Doxsey-Whitfield, E., and Mills, J.: Development of new open and free multi-temporal global population grids at 250 m resolution, *Geospatial Data in a Changing World*, Association of Geographic Information Laboratories in Europe (AGILE), ISBN 978-90-816960-6-7, 2016.
- Global Energy Monitor: Global Coal Mine Tracker, <https://globalenergymonitor.org/projects/global-coal-mine-tracker/> (last access: June 2024), 2022a.
- Global Energy Monitor: Global Coal Plant Tracker, <https://globalenergymonitor.org/projects/global-coal-plant-tracker/> (last access: June 2024), 2022b.
- Global Energy Monitor: Global Gas Plant Tracker, <https://globalenergymonitor.org/projects/global-gas-plant-tracker/> (last access: June 2024), 2022c.
- Global Energy Monitor: Global steel plant tracker, <https://globalenergymonitor.org/projects/global-steel-plant-tracker/> (last access: June 2024), 2022d.
- Guevara, M., Enciso, S., Tena, C., Jorba, O., Dellaert, S., Denier van der Gon, H., and Pérez García-Pando, C.: A global catalogue of CO₂ emissions and co-emitted species from power plants, including high-resolution vertical and temporal profiles, *Earth Syst. Sci. Data*, 16, 337–373, <https://doi.org/10.5194/essd-16-337-2024>, 2024.
- Hoesly, R. M., Smith, S. J., Feng, L., Klimont, Z., Janssens-Maenhout, G., Pitkanen, T., Seibert, J. J., Vu, L., Andres, R. J., Bolt, R. M., Bond, T. C., Dawidowski, L., Kholod, N., Kurokawa, J.-I., Li, M., Liu, L., Lu, Z., Moura, M. C. P., O'Rourke, P. R., and Zhang, Q.: Historical (1750–2014) anthropogenic emissions of reactive gases and aerosols from the Community Emissions Data System (CEDS), *Geosci. Model Dev.*, 11, 369–408, <https://doi.org/10.5194/gmd-11-369-2018>, 2018.
- IEA-EDGAR CO₂: A component of the EDGAR (Emissions Database for Global Atmospheric Research) Community GHG database version 8.0 (2023) including or based on data from IEA (2022) Greenhouse Gas Emissions from Energy, <http://www.iea.org/data-and-statistics> (last access: June 2024), 2023.
- Jalkanen, J.-P., Johansson, L., Kukkonen, J., Brink, A., Kalli, J., and Stipa, T.: Extension of an assessment model of ship traffic exhaust emissions for particulate matter and carbon monoxide, *Atmos. Chem. Phys.*, 12, 2641–2659, <https://doi.org/10.5194/acp-12-2641-2012>, 2012.
- Janssens-Maenhout, G., Crippa, M., Guizzardi, D., Muntean, M., Schaaf, E., Dentener, F., Bergamaschi, P., Pagliari, V., Olivier, J. G. J., Peters, J. A. H. W., van Aardenne, J. A., Monni, S., Doering, U., Petrescu, A. M. R., Solazzo, E., and Oreggioni, G. D.: EDGAR v4.3.2 Global Atlas of the three major greenhouse gas emissions for the period 1970–2012, *Earth Syst. Sci. Data*, 11, 959–1002, <https://doi.org/10.5194/essd-11-959-2019>, 2019.
- Jiang, J., Ye, B., and Liu, J.: Peak of CO₂ emissions in various sectors and provinces of China: Recent progress and avenues for further research, *Renew. Sust. Energ. Rev.*, 112, 813–833, <https://doi.org/10.1016/j.rser.2019.06.024>, 2019.
- Johansson, L., Jalkanen, J.-P., and Kukkonen, J.: Global assessment of shipping emissions in 2015 on a high spatial and temporal resolution, *Atmos. Environ.*, 167, 403–415, <https://doi.org/10.1016/j.atmosenv.2017.08.042>, 2017.
- Kuenen, J., Dellaert, S., Visschedijk, A., Jalkanen, J.-P., Super, I., and Denier van der Gon, H.: CAMS-REG-v4: a state-of-the-art high-resolution European emission inventory for air quality modelling, *Earth Syst. Sci. Data*, 14, 491–515, <https://doi.org/10.5194/essd-14-491-2022>, 2022.
- Kuramochi, T., Roelfsema, M., Hsu, A., Lui, S., Weinfurter, A., Chan, S., Hale, T., Clapper, A., Chang, A., and Höhne, N.: Beyond national climate action: the impact of region, city, and business commitments on global greenhouse gas emissions, *Clim. Pol.*, 20, 275–291, <https://doi.org/10.1080/14693062.2020.1740150>, 2020.
- Melchiorri, M.: The global human settlement layer sets a new standard for global urban data reporting with the urban centre database, *Front. Environ. Sci.*, 10, <https://doi.org/10.3389/fenvs.2022.1003862>, 2022.
- Melchiorri, M., Freire, S., Schiavina, M., Florczyk, A., Corbane, C., Maffeni, L., Pesaresi, M., Politis, P., Szabo, F., Ehrlich, D., Tommasi, P., Airaghi, D., Zanchetta, L., and Kemper, T.: The Multi-temporal and Multi-dimensional Global Urban Centre Database to Delineate and Analyse World Cities, *Sci. Data*, 11, 82, <https://doi.org/10.1038/s41597-023-02691-1>, 2024.
- NOAA-NGDC: Visible Infrared Imaging Radiometer Suite (VIIRS), <https://www.ngdc.noaa.gov/eog/viirs.html> (last access: July 2023), 2017.
- Pesaresi, M. and Politis, P.: GHS-BUILT-S R2023A – GHS built-up surface grid, derived from Sentinel2 composite and Landsat, multitemporal (1975–2030), European Commission, Joint Research Centre (JRC) [data set], <https://doi.org/10.2905/9F06F36F-4B11-47EC-ABB0-4F8B7B1D72EA>, 2023.
- Schiavina, M., Melchiorri, M., and Pesaresi, M.: GHS-SMOD R2023A – GHS settlement layers, application of the Degree of Urbanisation methodology (stage I) to GHS-POP R2023A and GHS-BUILT-S R2023A, multitemporal (1975–2030), European Commission, Joint Research Centre (JRC) [data set], <https://doi.org/10.2905/A0DF7A6F-49DE-46EA-9BDE-563437A6E2BA>, 2023a.
- Schiavina, M., Freire, S., Carioli, A., and MacManus, K.: GHS-POP R2023A – GHS population grid multitemporal (1975–2030). European Commission, Joint Research Centre (JRC) [data set], <https://doi.org/10.2905/2FF68A52-5B5B-4A22-8F40-C41DA8332CFE>, 2023b.
- Spinoni, J., Vogt, J. V., Barbosa, P., Dosio, A., McCormick, N., Bigano, A., and Fussler, H. M.: Changes: Changes of heating and cooling degree-days in Europe from 1981 to 2100, *Int. J. Climatol.*, 38, e191–e208, <https://doi.org/10.1002/joc.5362>, 2018.

- Thunis, P., Kuenen, J., Pisoni, E., Bessagnet, B., Banja, M., Gawuc, L., Szymankiewicz, K., Guizardi, D., Crippa, M., Lopez-Aparicio, S., Guevara, M., De Meij, A., Schindlbacher, S., and Clappier, A.: Emission ensemble approach to improve the development of multi-scale emission inventories, *Geosci. Model Dev.*, 17, 3631–3643, <https://doi.org/10.5194/gmd-17-3631-2024>, 2024.
- Ummel, K.: Carma Revisited: An Updated Database of Carbon Dioxide Emissions from Power Plants Worldwide, Center for Global Development Working Paper No. 304, <https://doi.org/10.2139/ssrn.2226505>, 2012.
- US EIA: US Coal mines, <https://atlas.eia.gov/datasets/eia::coal-mines-1/explore> (last access: June 2024), 2022a.
- US EIA: US Energy Atlas, <https://atlas.eia.gov/datasets/eia::power-plants/explore?location=41.629235%2C-118.496000%2C3.79> (last access: June 2024), 2022b.
- USGS: USGS Mineral Resources On-Line Spatial Data, <http://mrdata.usgs.gov/> (last access: January 2019), 2019.
- Van Damme, M., Clarisse, L., Whitburn, S., Hadji-Lazarou, J., Hurtmans, D., Clerbaux, C., and Coheur, P.-F.: Industrial and agricultural ammonia point sources exposed, *Nature*, 564, 99–103, <https://doi.org/10.1038/s41586-018-0747-1>, 2018.
- Wang, C., Corbett, J., and Firestone, J.: Improving Spatial Representation of Global Ship Emissions Inventories, *Environ. Sci. Technol.*, 42, 193–199, <https://doi.org/10.1021/es0700799>, 2008.
- World Bank: Global Gas Flaring Tracker Report, <https://www.worldbank.org/en/programs/gasflaringreduction/global-flaring-data> (last access: August 2023), 2023.
- World Resources Institute: Global Power Plant Database, Global Energy Observatory, Google, KTH Royal Institute of Technology in Stockholm, Enipedia, <http://resourcewatch.org/> (last access: June 2024), 2018.
- WRI: Global Power Plant Database v1.3.0, <https://datasets.wri.org/dataset/globalpowerplantdatabase> (last access: June 2024), 2021.
- Zhang, X., Geng, Y., Shao, S., Dong, H., Wu, R., Yao, T., and Song, J.: How to achieve China's CO₂ emission reduction targets by provincial efforts? – An analysis based on generalized Divisia index and dynamic scenario simulation, *Renew. Sust. Energ. Rev.*, 127, 109892, <https://doi.org/10.1016/j.rser.2020.109892>, 2020.